Electronic
Research Archive

https://www.aimspress.com/journal/era

ERA, 34(8): 5525–5545.
DOI: 10.3934/era.2026247
Received: 26 March 2026
Revised: 09 June 2026
Accepted: 16 June 2026
Published: 30 June 2026

Research article

Estimation and numerical approximation for a type of time fractional delay diffusion equation

Chaoqin Yi[1], **Peiyan Li**[2] **and Wei Gu**[3,*]

[1] Department of General Education, Shanghai Urban Construction Vocational College, Shanghai 201415, China
[2] School of Mathematics and Statistics, Central China Normal University, Wuhan 430079, China
[3] School of Statistics and Mathematics, Zhongnan University of Economics and Law, Wuhan 430073, China

* **Correspondence:** Email: wei_gu@zuel.edu.cn.

Abstract: An improved single-component Metropolis–Hastings (ISC–MH) algorithm for estimating a kind of time fractional delay diffusion equation (FDDE) is provided. We introduce the symmetric proposal distribution for generating the candidate point of each parameter to obtain the ISC–MH algorithm. To estimate the unknown parameter of the FDDE, firstly, we construct the compact difference scheme to numerically discretize the FDDE. Then the ISC–MH algorithm is used to estimate the fractional order, the diffusion coefficient, and the time delay in the system of the FDDE simultaneously. Finally, some simulation tests of two examples are provided to validate the performance of the algorithms.

Keywords: fractional order; time delay; the compact difference scheme; improved single-component Metropolis–Hastings algorithm

1. Introduction

In the past few years, fractional differential equation models have been used to model problems in the fields of finance, physics, bioecology, and so on [1–3]. However, it is hard to obtain closed–form solutions of fractional differential equations. Many numerical approximation methods have been provided to solve fractional differential equation models, such as finite differencing [4, 5], the finite element method [6, 7], the decomposition method [8], the collocation method [9], and so on.

However, there is weak singularity at time $t = 0$. To solve this problem, Stynes et al. [10], Shen et al. [11], and Kopteva [12] introduced graded meshes to refine the discretization near the initial time and obtained the optimal covergence rates. Some studies focused on local error analysis rather than global error analysis [13–15]. Li et al. [16] and Liao et al. [17] developed discrete fractional Gronwall inequalities for L1–type schemes, enabling unconditional stability and optimal error estimates without restrictive smoothness assumptions. These tools have been extended to nonlinear and delay problems [18–22]. Pang et al. [23] introduced fractional physics–informed neural networks (fPINNs), the foundational work that extends physics–informed nerual networks (PINNs) to fractional partial differential equations (PDEs). Shi et al. [24] proposed a fast L1–based fPINN method (FL1–fPINN) using graded meshes for high-dimensional time-fractional reaction–diffusion equations, integrating adaptive activation functions and hybrid constraints. It achieved significant gains in accuracy and efficiency for both forward and inverse problems. Zhang et al. [25] developed Laplace transform (LT)–PINNs, a framework that constructs the loss function via the Laplace transform to circumvent the difficulty of discretizing fractional derivatives. It outperforms conventional fPINNs in accuracy and computational speed, and can simultaneously identify the fractional order, convection coefficient, and diffusion coefficient.

In recent years, the studies concerned with the estimation of the unknown parameter of the fractional diffusion equation have attracted more and more researchers. However, few papers have been devoted to estimating the fractional differential equation model with time delay. The Levenberg–Marquardt scheme was considered by Yu et al. [26] to estimate the order of a fractional Stokes model. Malti et al. [27] used the simplified refined instrumental variable method to estimate the orders and the coefficients of the fractional model. Zhang et al. [28] considered a two–stage algorithm to estimate the orders and coefficients of the fractional system. Meanwhile, the extended maximum likelihood method [29], the sensitivity analysis method [30], the Bayesian method [31–36], and an estimation method based on Gaussian processes [37, 38] have been considered for estimating the problem of fractional differential equation models with noisy observations.

Despite these advances, several challenges remain. First, most existing parameter estimation methods for fractional diffusion equations focus on models without time delays; simultaneous estimation of the fractional order, diffusion coefficient, and time delay has been seldom studied. Second, gradient–based or sensitivity–based methods can become trapped in local optima when applied to fractional systems, where the objective function may be highly non-convex. Third, while Bayesian methods provide a natural framework for uncertainty quantification, their application to fractional delay models is still limited. These considerations motivate the present work, in which we develop an improved single–component Metropolis–Hastings (ISC–MH) algorithm that can efficiently handle the three parameter estimation problem in a fractional delay diffusion equation (FDDE) system.

The novelty of this paper lies not in the forward scheme itself, but in its application to the inverse problem specifically, namely the simultaneous estimation of the fractional order, the diffusion coefficient, and the time delay in an FDDE system using the ISC-MH algorithm. To our knowledge, this inverse problem has not been addressed in prior work, and the ISC-MH algorithm with symmetric independent proposal distributions tailored for the delay parameter is new. To estimate the unknown parameter of the FDDE, we construct the compact difference scheme to numerically discretize the FDDE. Then the ISC-MH algorithm is constructed to estimate the unknown parameter of the model. Finally, some simulation tests of two examples are provided to validate the effectiveness of the considered algorithm in the paper.

We organize this paper as follows. Section 2 introduces the model, then the compact difference scheme is considered to discretize the FDDE. Section 3 applies the ISC–MH algorithm to solve the inverse problem of the model. Section 4 considers some numerical examples to test the validity of the provided schemes for forward problem of the system of the FDDE. Section 5 mainly considers the performance of ISC–MH algorithm for the estimation problem of the FDDE system. Section 6 provides a short remark on this paper.

2. The FDDE and the compact difference scheme

We construct a high–order compact difference scheme to obtain the numerical solution of a kind of FDDE.

2.1. Fractional delay diffusion equation

The following FDDE is considered:

$$\frac{\partial^\alpha u}{\partial t^\alpha} = Q\frac{\partial^2 u(x,t)}{\partial x^2} + f(u(x,t), u(x,t-s), x, t), \quad (x,t) \in (0,1)\times(0,T], \tag{2.1}$$

$$u(x,t) = \phi(x,t), \quad x \in [0,1], \quad t \in [-s,0], \tag{2.2}$$

$$u(0,t) = \beta_1(t), \quad u(1,t) = \beta_2(t), \quad t \in [0,T], \tag{2.3}$$

where $s > 0$ and $Q > 0$ represent the delay term and diffusion coefficient, respectively; $\phi(\cdot), \beta_1(\cdot)$, and $\beta_2(\cdot)$ are known functions. Fractional partial derivative $\frac{\partial^\alpha u}{\partial t^\alpha}$ $(0 < \alpha < 1)$ is defined as follows:

$$\frac{\partial^\alpha u}{\partial t^\alpha} = \frac{1}{\Gamma(1-\alpha)}\int_0^t (t-\xi)^{-\alpha}\frac{\partial u(x,\xi)}{\partial \xi}d\xi, \tag{2.4}$$

where $\Gamma(\cdot)$ represents the Gamma function.

If $\theta = (\alpha, Q, s)$ is a known parameter, many methods have been provided to numerically solve (2.1)–(2.3), such as [39,40] and the references therein. In practice, we may estimate the unknown parameter θ from some given observations. The observations may be observed with or without measurement error at some continuous or discrete time points. For example, assume that we have the following observations observed at $t = T$:

$$y(x) = u(x,T), \quad 0 < x \leq 1. \tag{2.5}$$

Assume $F : \theta \mapsto u(x,T;\theta)$ be an operator with an unknown parameter $\theta = (\alpha, Q, s)$, then the inverse problem is to obtain θ from (2.1)–(2.3) together with the following:

$$F(\theta) = y, \tag{2.6}$$

where the ISC-MH algorithm will be considered to estimate the unknown parameter $\theta = (\alpha, Q, s)$.

2.2. The compact difference scheme

We introduce the compact difference scheme to solve (2.1)–(2.3) in this section.

Take $x_i = ih, i = 0, 1, \cdots, M$, and $t_k = k\tau, k = 0, 1, \cdots, N$, where $h = 1/M, \tau = s/n$ (assume that M and n are two positive integers), and $N = [T/\tau]$. Define $\Omega_{h\tau} = \Omega_h \times \Omega_\tau$, where $\Omega_h = \{x_i | 0 \le i \le M\}$, $\Omega_\tau = \{t_k | -n \le k \le N\}$. Introduce $U_i^k = u(x_i, t_k), 0 \le i \le M, -n \le k \le N$. Let

$$\mathcal{V} = \{v_i^k | 0 \le i \le M, -n \le k \le N\}$$

be the grid function space defined on $\Omega_{h\tau}$. We introduce the following:

$$\delta_x v_{i+1/2}^k = \frac{v_{i+1}^k - v_i^k}{h}, \delta_x^2 v_i^k = \frac{v_{i+1}^k - 2v_i^k + v_{i-1}^k}{h^2}, \mathcal{H} v_i^k = \frac{1}{12}(v_{i-1}^k + 10v_i^k + v_{i+1}^k),$$

$$\delta_t^\alpha v^k = \frac{\tau^{-\alpha}}{\Gamma(2-\alpha)}[d_0 v^k - \sum_{j=1}^{k-1}(d_{k-j-1} - d_{k-j})v^j - d_{k-1}v^0],$$

where $d_j = (j+1)^{1-\alpha} - j^{1-\alpha}, j \ge 0$.

Assume u_i^k to be the numerical solution of (2.1)–(2.3). One can easily get the following compact difference scheme by reference to [39]:

$$\mathcal{H}\delta_t^\alpha u_i^k = Q\delta_x^2 u_i^k + \mathcal{H} f(2u_i^{k-1} - u_i^{k-2}, u_i^{k-n}, x_i, t_k), 1 \le i \le M-1, 1 \le k \le N, \tag{2.7}$$

$$u_i^k = \phi(x_i, t_k), \ \ 0 \le i \le M, -n \le k \le 0, \tag{2.8}$$

$$u_0^k = \beta_1(t_k), \ \ u_M^k = \beta_2(t_k), \ \ 1 \le k \le N. \tag{2.9}$$

There are some results on the scheme in (2.7)–(2.9).

Theorem 1: Assume that $f(\cdot)$ in (2.1) satisfies the following inequality:

$$|f(t, u_1, v_1) - f(t, u_2, v_2)| \le L_1|u_1 - u_2| + L_2|v_1 - v_2|, \tag{2.10}$$

where $L_1 > 0$ and $L_2 > 0$ are two constants. There is a unique solution of the difference scheme (2.7)–(2.9).

Proof: The difference scheme of (2.7)–(2.9) can be rewritten into a linear tridiagonal system $\mathcal{M}u^k = L$, where L is the function of $u^j (j \le k-1)$, u_0^k and u_M^k, and is independent of u^k. If we assume that $\lambda = \tau^\alpha \Gamma(2-\alpha)$, we can see that $\mathcal{M} = tridiag(\frac{1}{12\lambda} - \frac{Q}{h^2}, \frac{10}{12\lambda} + \frac{2Q}{h^2}, \frac{1}{12\lambda} - \frac{Q}{h^2})$ is a strictly diagonally dominant coefficient matrix, and thus scheme (2.7)–(2.9) has a unique solution.

Denote $e_i^k = U_i^k - u_i^k, 0 \le i \le M, 0 \le k \le N$, where $U_i^k = u(x_i, t_k)$. The following can be obtained [39]:

$$\mathcal{H}\delta_t^\alpha e_i^k = Q\delta_x^2 e_i^k + \mathcal{H} q_i^k + R_i^k, 1 \le i \le M-1, 1 \le k \le N, \tag{2.11}$$

$$e_i^0 = 0, \ \ 0 \le i \le M, \tag{2.12}$$

$$e_0^k = 0, \quad e_M^k = 0, \quad 1 \le k \le N, \tag{2.13}$$

where $q_i^k = f(2U_i^{k-1} - U_i^{k-2}, U_i^{k-n}, x_i, t_k) - f(2u_i^{k-1} - u_i^{k-2}, u_i^{k-n}, x_i, t_k)$, and $R_i^k = O(\tau^{2-\alpha} + h^4)$.

Assume the following:

$$(u, v) = h \sum_{i=1}^{M-1} u_i v_i, \quad \|u\| = \sqrt{(u, u)}, \quad \|u\|_\infty = \max_{1\le i\le M-1} |u_i|,$$
$$\langle \delta_x u, \delta_x v\rangle = h \sum_{i=0}^{M-1} (\delta_x u_{i+\frac{1}{2}})(\delta_x v_{i+\frac{1}{2}}), \quad |\delta_x u|_1 = \sqrt{\langle \delta_x u, \delta_x u\rangle}.$$

Theorem 2: Assume that $f(\cdot)$ in (2.1) satisfies the same condition as Theorem 1, then $\{u_i^k | 0 \le i \le M, 0 \le k \le N\}$ will be the unique solution of (2.7)–(2.9), and we have

$$\|e^k\|_\infty \le C(\tau^{2-\alpha} + h^4), \quad 0 \le k \le N,$$

where C is a positive constant that is independent of h and τ.

Proof: If we multiply (2.11) by $h\delta_t^\alpha e_i^k$ and sum up for i from 1 to $M-1$, we obtain

$$h \sum_{i=1}^{M-1} (\mathcal{H}\delta_t^\alpha e_i^k)(\delta_t^\alpha e_i^k) = Qh \sum_{i=1}^{M-1} (\delta_x^2 e_i^k)(\delta_t^\alpha e_i^k) + h \sum_{i=1}^{M-1} (\mathcal{H}q_i^k)(\delta_t^\alpha e_i^k) + h \sum_{i=1}^{M-1} (R_i^k)(\delta_t^\alpha e_i^k), \tag{2.14}$$

where $1 \le i \le M-1, 1 \le k \le N$. For each term of (2.14), we have

$$\begin{aligned}
&h \sum_{i=1}^{M-1} (\mathcal{H}\delta_t^\alpha e_i^k)(\delta_t^\alpha e_i^k) = h \sum_{i=1}^{M-1} \tfrac{1}{12}(\delta_t^\alpha e_{i-1}^k + 10\delta_t^\alpha e_i^k + \delta_t^\alpha e_{i+1}^k)(\delta_t^\alpha e_i^k)\\
&= \tfrac{h}{24} \sum_{i=1}^{M-1} [2(\delta_t^\alpha e_{i-1}^k)(\delta_t^\alpha e_i^k) + 20(\delta_t^\alpha e_i^k)^2 + 2(\delta_t^\alpha e_{i+1}^k)(\delta_t^\alpha e_i^k)]\\
&\ge \tfrac{h}{24} \sum_{i=1}^{M-1} [20(\delta_t^\alpha e_i^k)^2 - (\delta_t^\alpha e_{i-1}^k)^2 - 2(\delta_t^\alpha e_i^k)^2 - (\delta_t^\alpha e_{i+1}^k)^2]\\
&\ge \tfrac{2}{3}\|\delta_t^\alpha e^k\|^2.
\end{aligned} \tag{2.15}$$

By the discrete Green formula, we have

$$\begin{aligned}
&Qh \sum_{i=1}^{M-1} (\delta_x^2 e_i^k)(\delta_t^\alpha e_i^k) = -Qh \sum_{i=0}^{M-1} (\delta_x e_{i+1/2}^k)(\delta_t^\alpha \delta_x e_{i+1/2}^k)\\
&= -\tfrac{Q}{\lambda} h \sum_{i=0}^{M-1} (\delta_x e_{i+1/2}^k)[\delta_x e_{i+1/2}^k - \sum_{j=1}^{k-1} (d_{k-j-1} - d_{k-j})\delta_x e_{i+1/2}^j - d_{k-1}\delta_x e_{i+1/2}^0]\\
&= -\tfrac{Q}{\lambda}\{|\delta_x e^k|_1^2 - \sum_{j=1}^{k-1} (d_{k-j-1} - d_{k-j})\langle \delta_x e^k, \delta_x e^j\rangle - d_{k-1}\langle \delta_x e^k, \delta_x e^0\rangle\}\\
&\le -\tfrac{Q}{\lambda}\{|\delta_x e^k|_1^2 - \sum_{j=1}^{k-1} (d_{k-j-1} - d_{k-j})\tfrac{|\delta_x e^k|_1^2 + |\delta_x e^j|_1^2}{2} - d_{k-1}\tfrac{|\delta_x e^k|_1^2 + |\delta_x e^0|_1^2}{2}\}\\
&= -\tfrac{Q}{\lambda}\{\tfrac{|\delta_x e^k|_1^2}{2} - \sum_{j=1}^{k-1} (d_{k-j-1} - d_{k-j})\tfrac{|\delta_x e^j|_1^2}{2}\},
\end{aligned} \tag{2.16}$$

where $\lambda = \tau^\alpha \Gamma(2-\alpha)$.

From the Cauchy–Schwarz inequality, (2.10), and Lemma 4 in [39], one can obtain

$$\begin{aligned} h\sum_{i=1}^{M-1}(\mathcal{H}q_i^k)(\delta_t^\alpha e_i^k) &\le \frac{\varepsilon}{2}\|\delta_t^\alpha e^k\|^2 + \frac{1}{2\varepsilon}h\sum_{i=1}^{M-1}(\mathcal{H}[c_0|2e_i^{k-1}-e_i^{k-2}| + c_1|e_i^{k-n}|])^2 \\ &\le \frac{\varepsilon}{2}\|\delta_t^\alpha e^k\|^2 + \frac{1}{2\varepsilon}h\sum_{i=1}^{M-1}(c_0|2e_i^{k-1}-e_i^{k-2}| + c_1|e_i^{k-n}|)^2 \\ &\le \frac{\varepsilon}{2}\|\delta_t^\alpha e^k\|^2 + \frac{1}{\varepsilon}c_0^2 h\sum_{i=1}^{M-1}(2e_i^{k-1}-e_i^{k-2})^2 + \frac{1}{\varepsilon}c_1^2 h\sum_{i=1}^{M-1}(e_i^{k-n})^2 \\ &\le \frac{\varepsilon}{2}\|\delta_t^\alpha e^k\|^2 + \frac{8c_0^2}{\varepsilon}(\|e^{k-1}\|^2 + \|e^{k-2}\|^2) + \frac{c_1^2}{\varepsilon}\|e^{k-n}\|^2, \end{aligned} \tag{2.17}$$

and

$$h\sum_{i=1}^{M-1}(R_i^k)(\delta_t^\alpha e_i^k) \quad \le \frac{1}{2\varepsilon}\|R^k\|^2 + \frac{\varepsilon}{2}\|\delta_t^\alpha e^k\|^2. \tag{2.18}$$

By inserting (2.15)–(2.18) into (2.14), and letting $\varepsilon = 2/3$, one obtains

$$\begin{aligned} |\delta_x e^k|_1^2 &\le \sum_{j=1}^{k-1}(d_{k-j-1}-d_{k-j})|\delta_x e^j|_1^2 + \frac{24\lambda c_0^2}{Q}(\|e^{k-1}\|^2 + \|e^{k-2}\|^2) + \frac{3\lambda c_1^2}{Q}\|e^{k-n}\|^2 + \frac{3\lambda}{2Q}\|R^k\|^2 \\ &\le \sum_{j=1}^{k-1}(d_{k-j-1}-d_{k-j})|\delta_x e^j|_1^2 + \frac{4\lambda c_0^2}{Q}(|\delta_x e^{k-1}|_1^2 + |\delta_x e^{k-2}|_1^2) + \frac{\lambda c_1^2}{2Q}|\delta_x e^{k-n}|_1^2 + \frac{3\lambda}{2Q}\|R^k\|^2, \end{aligned} \tag{2.19}$$

where Lemma 5 in [39] is used.

Write $C' = \frac{\lambda}{Q}\max\{4c_0^2, c_1^2/2, 3/2\}$, and notice that $R_i^k = O(\tau^{2-\alpha}+h^4)$, by Lemma 6 in [39], one obtains

$$|\delta_x e^k|_1^2 \le C'\exp(3C'+1)(\tau^{2-\alpha}+h^4)^2 = C''(\tau^{2-\alpha}+h^4)^2,$$

where $C'' = C'\exp(3C'+1)$ is a positive constant independent of h and τ. We then have

$$\|e^k\|_\infty \le \sqrt{C''(\tau^{2-\alpha}+h^4)^2}/2 \doteq C(\tau^{2-\alpha}+h^4).$$

The proof is complete.

As for the stability of the difference scheme (2.7)–(2.9), we introduce the following problem:

$$\mathcal{H}\frac{\partial^\alpha v}{\partial t^\alpha} = Q\frac{\partial^2 v(x,t)}{\partial x^2} + \mathcal{H}f(v(x,t), v(x,t-s), x, t), \quad (x,t) \in (0,1)\times(0,T], \tag{2.20}$$

$$v(x,t) = \phi(x,t) + \psi(x,t), \quad x \in [0,1], \quad t \in [-s,0], \tag{2.21}$$

$$v(0,t) = \gamma_1(t), \quad v(1,t) = \gamma_2(t), \quad t \in (0,T], \tag{2.22}$$

where $\psi(x,t)$ is the perturbation caused by $\phi(x,t)$. We can obtain the following difference scheme solving for (2.20)–(2.22):

$$\mathcal{H}\delta_t^\alpha v_i^k = Q\delta_x^2 v_i^k + \mathcal{H}f(2v_i^{k-1} - v_i^{k-2}, v_i^{k-n}, x_i, t_k), \tag{2.23}$$

$$v_i^k = \phi(x_i, t_k) + \psi_i^k, \;\; 0 \le i \le M, -n \le k \le 0, \tag{2.24}$$

$$v_0^k = \gamma_1(t_k), \;\; v_M^k = \gamma_2(t_k), \;\; 1 \le k \le N. \tag{2.25}$$

Introducing

$$\omega_i^k = v_i^k - u_i^k, \;\; 0 \le i \le M, -n \le k \le N. \tag{2.26}$$

Theorem 3: Under the same condition as Theorem 2, the difference scheme (2.7)–(2.9) is stable with respect to the initial perturbation of ψ_i^k, that is $\|\omega^k\|_\infty \le \hat{C} \max\limits_{-n\le j\le 0} |\psi^j|_1$, where $\hat{C}$ is a positive constant independent of h and τ.

Proof: Subtracting (2.23)–(2.25) from (2.7)–(2.9), respectively, we can obtain the following equations:

$$\mathcal{H}\delta_t^\alpha \omega_i^k = Q\delta_x^2\omega_i^k + \mathcal{H}p_i^k, \tag{2.27}$$

$$\omega_i^k = \psi_i^k, \;\; 0 \le i \le M, -n \le k \le 0, \tag{2.28}$$

$$\omega_0^k = 0, \;\; \omega_M^k = 0, \;\; 1 \le k \le N, \tag{2.29}$$

where $p_i^k = f(2v_i^{k-1} - v_i^{k-2}, v_i^{k-n}, x_i, t_k) - f(2u_i^{k-1} - u_i^{k-2}, u_i^{k-n}, x_i, t_k)$.

Multiplying $h\delta_t^\alpha \omega_i^k$ on both sides of (2.27) and summing up for i from 1 to $M-1$, we obtain

$$\begin{aligned} &h\sum_{i=1}^{M-1}(\mathcal{H}\delta_t^\alpha\omega_i^k)(\delta_t^\alpha\omega_i^k) = Qh\sum_{i=1}^{M-1}(\delta_x^2\omega_i^k)(\delta_t^\alpha\omega_i^k) + h\sum_{i=1}^{M-1}(\mathcal{H}p_i^k)(\delta_t^\alpha\omega_i^k), \\ &1 \le i \le M-1, 0 \le k \le N-1. \end{aligned} \tag{2.30}$$

Then each term of (2.30) will be estimated. From the discrete Green formula and inequality $-(a+b)^2 \ge -2(a^2+b^2)$, we have

$$\begin{aligned} &h\sum_{i=1}^{M-1}(\mathcal{H}\delta_t^\alpha\omega_i^k)(\delta_t^\alpha\omega_i^k) = \|\delta_t^\alpha\omega_i^k\|^2 + \frac{h^2}{12}h\sum_{i=1}^{M-1}(\delta_x^2(\delta_t^\alpha\omega_i^k))(\delta_t^\alpha\omega_i^k) \\ &= \|\delta_t^\alpha\omega_i^k\|^2 - \frac{h^2}{12}\|\delta_x\delta_t^\alpha\omega_i^k\|^2 \ge \frac{2}{3}\|\delta_t^\alpha\omega_i^k\|^2. \end{aligned} \tag{2.31}$$

From the discrete Green formula and the inequality $-ab \ge -(a^2+b^2)/2$, we have

$$\begin{aligned} &Qh\sum_{i=1}^{M-1}(\delta_x^2\omega_i^k)(\delta_t^\alpha\omega_i^k) = -Qh\sum_{i=0}^{M-1}(\delta_x\omega_{i+1/2}^k)(\delta_t^\alpha\delta_x\omega_{i+1/2}^k) \\ &= -\frac{Q}{\lambda}h\sum_{i=0}^{M-1}(\delta_x\omega_{i+1/2}^k)[\delta_x\omega_{i+1/2}^k - \sum_{j=1}^{k-1}(d_{k-j-1} - d_{k-j})\delta_x\omega_{i+1/2}^j - d_{k-1}\delta_x\omega_{i+1/2}^0] \\ &= -\frac{Q}{\lambda}\{|\delta_x\omega^k|_1^2 - \sum_{j=1}^{k-1}(d_{k-j-1} - d_{k-j})\langle\delta_x\omega^k, \delta_x\omega^j\rangle - d_{k-1}\langle\delta_x\omega^k, \delta_x\omega^0\rangle\} \\ &\le -\frac{Q}{\lambda}\{|\delta_x\omega^k|_1^2 - \sum_{j=1}^{k-1}(d_{k-j-1} - d_{k-j})\frac{|\delta_x\omega^k|_1^2 + |\delta_x\omega^j|_1^2}{2} - d_{k-1}\frac{|\delta_x\omega^k|_1^2 + |\delta_x\omega^0|_1^2}{2}\} \\ &= -\frac{Q}{\lambda}\{\frac{|\delta_x\omega^k|_1^2}{2} - \sum_{j=1}^{k-1}(d_{k-j-1} - d_{k-j})\frac{|\delta_x\omega^j|_1^2}{2} - d_{k-1}\frac{|\delta_x\omega^0|_1^2}{2}\}. \end{aligned} \tag{2.32}$$

From the Cauchy–Schwarz inequality, Lemma 4 in [39] and (2.10), we have

$$
\begin{aligned}
&h\sum_{i=1}^{M-1}(\mathcal{H}p_i^k)(\delta_t^\alpha\omega_i^k) \le \tfrac{1}{2\varepsilon}\|\delta_t^\alpha\omega_i^k\|^2 + \tfrac{\varepsilon}{2}h\sum_{i=1}^{M-1}(\mathcal{H}[c_0|2\omega_i^{k-1}-\omega_i^{k-2}| + c_1|\omega_i^{k-n}|])^2\\
&\le \tfrac{1}{2\varepsilon}\|\delta_t^\alpha\omega_i^k\|^2 + \tfrac{\varepsilon}{2}h\sum_{i=1}^{M-1}(c_0|2\omega_i^{k-1}-\omega_i^{k-2}| + c_1|\omega_i^{k-n}|)^2\\
&\le \tfrac{1}{2\varepsilon}\|\delta_t^\alpha\omega_i^k\|^2 + \varepsilon c_0^2 h\sum_{i=1}^{M-1}(2\omega_i^{k-1}-\omega_i^{k-2})^2 + \varepsilon c_1^2 h\sum_{i=1}^{M-1}(\omega_i^{k-n})^2\\
&\le \tfrac{1}{2\varepsilon}\|\delta_t^\alpha\omega_i^k\|^2 + 8\varepsilon c_0^2(\|\omega^{k-1}\|^2 + \|\omega^{k-2}\|^2) + \varepsilon c_1^2\|\omega^{k-n}\|^2.
\end{aligned}
\tag{2.33}
$$

Inserting (2.31)–(2.33) into (2.30), and taking $\varepsilon = 3/4$ in (2.33), we obtain

$$
\begin{aligned}
&\tfrac{Q}{2\lambda}|\delta_x\omega^k|_1^2 \le \tfrac{Q}{2\lambda}\sum_{j=1}^{k-1}(d_{k-j-1}-d_{k-j})|\delta_x\omega^j|_1^2\\
&+ \tfrac{Q}{2\lambda}d_{k-1}|\delta_x\omega^0|_1^2 + 6c_0^2(\|\omega^{k-1}\|^2 + \|\omega^{k-2}\|^2) + \tfrac{3}{4}c_1^2\|\omega^{k-n}\|^2\\
&\le \tfrac{Q}{2\lambda}\sum_{j=1}^{k-1}(d_{k-j-1}-d_{k-j})|\delta_x\omega^j|_1^2 + \tfrac{Q}{2\lambda}d_{k-1}|\delta_x\omega^0|_1^2\\
&+ c_0^2(|\delta_x\omega^{k-1}|_1^2 + |\delta_x\omega^{k-2}|_1^2) + \tfrac{1}{8}c_1^2|\delta_x\omega^{k-n}|_1^2,
\end{aligned}
\tag{2.34}
$$

where Lemma 5 in [39] has been used.

Multiplying (2.34) by $\frac{2\lambda}{Q}$, we have

$$
\begin{aligned}
&|\delta_x\omega^k|_1^2 \le \sum_{j=1}^{k-1}(d_{k-j-1}-d_{k-j})|\delta_x\omega^j|_1^2 + |\delta_x\omega^0|_1^2\\
&+\tfrac{2\lambda}{Q}c_0^2(|\delta_x\omega^{k-1}|_1^2 + |\delta_x\omega^{k-2}|_1^2) + \tfrac{\lambda}{4Q}c_1^2|\delta_x\omega^{k-n}|_1^2.
\end{aligned}
\tag{2.35}
$$

We write

$$
C_k = \max\{\frac{2\Gamma(2-\alpha)}{Q}c_0^2, \frac{\Gamma(2-\alpha)}{2Q}c_1^2\} > 0.
$$

Noticing that $\lambda = \tau^\alpha\Gamma(2-\alpha)$, for $0 < \tau < 1$, we have $\tau^\alpha < 1$. Then from (2.35), we obtain

$$
|\delta_x\omega^k|_1^2 \le \sum_{j=1}^{k-1}(d_{k-j-1}-d_{k-j})|\delta_x\omega^j|_1^2 + |\delta_x\omega^0|_1^2 + C_k(|\delta_x\omega^{k-1}|_1^2 + |\delta_x\omega^{k-2}|_1^2 + |\delta_x\omega^{k-n}|_1^2). \tag{2.36}
$$

From Lemmas 2 and 6 in [39], we have

$$
\begin{aligned}
&|\delta_x\omega^k|_1^2 \le (3C_k+1)\exp(3C_k+1)\max_{-n\le j\le 0}|\delta_x\omega^j|_1^2\\
&\le (3C_k+1)\exp(3C_k+1)\max_{-n\le j\le 0}|\delta_x\psi^j|_1^2.
\end{aligned}
\tag{2.37}
$$

From Lemma 5 in [39], we have

$$
\|\omega^k\|_\infty \le \hat{C}\max_{-n\le j\le 0}|\psi^j|_1.
$$

The proof is complete.

3. The ISC–MH algorithm

Assume that with the following observations to be observed with measurement error:

$$y = F(\theta) + \varepsilon, \tag{3.1}$$

where $\varepsilon \sim N(0, \sigma^2)$, (however, the proposed ISC-MH method is expected to be robust under non-Gaussian or heavy-tailed noise (e.g., Laplace or Student's t); a systematic investigation under various noise distributions is an important direction for future work), and $F(\theta)$ is the numerical solution of (2.1)–(2.3). We will estimate the unknown parameter $\theta = (\alpha, Q, s)$ from the observations governed by (3.1).

From the Bayes theorem, the posterior probability density function (PPDF) is

$$p(\theta|y) \propto p(y|\theta)p(\theta), \tag{3.2}$$

where $p(y|\theta)$ is the likelihood function of the observations $y = (y_1, y_2, \cdots, y_R)$, and $p(\theta)$ is the prior density. From (3.1), the PPDF of θ can be approximated by

$$p(\theta|y) \propto p(\theta) \prod_{r=1}^{R} N(y_r; F(\theta), \sigma^2), \tag{3.3}$$

where R denotes the number of observations, $N(\cdot; F(\theta), \sigma^2)$ denotes the normal distribution with a mean of $F(\theta)$ and a variance of σ^2.

We improve the traditional single–component Metropoli–Hastings algorithm through introducing the symmetric normal distribution with updated mean and fixed variance as the proposal distribution. The ISC-MH algorithm will be constructed to estimate $\theta = (\theta_1, \theta_2, \theta_3) = (\alpha, Q, s)$ as follows.

Initialize $\theta_0 = (\theta_1^{(0)}, \theta_2^{(0)}, \theta_3^{(0)})$.

For $t = 1 : N_{sim}$:

1) Let $\theta = (\theta_1, \theta_2, \theta_3) = (\theta_1^{(t-1)}, \theta_2^{(t-1)}, \theta_3^{(t-1)})$.

2) Simulate $\theta_1^* \sim N(\theta_1^{(t-1)}, \sigma_1^2)$.

3) Let $\theta^* = (\theta_1^*, \theta_2^{(t-1)}, \theta_3^{(t-1)})$, and compute

$$\varsigma_1(\theta, \theta^*) = min\{1, \frac{p(y|\theta_1^*, \theta_2, \theta_3)p(\theta^*, \theta_2, \theta_3)}{p(y|\theta_1, \theta_2, \theta_3)p(\theta_1, \theta_2, \theta_3)}\}. \tag{3.4}$$

4) Generate $U_1 \sim U(0, 1)$, if $U_1 \le \varsigma_1(\theta, \theta^*)$ and set $\theta = \theta^*$; otherwise, keep θ unchanged.

5) Simulate $\theta_2^* \sim N(\theta_2^{(t-1)}, \sigma_2^2)$.

6) Let $\theta^* = (\theta_1, \theta_2^*, \theta_3^{(t-1)})$, and compute

$$\varsigma_2(\theta, \theta^*) = min\{1, \frac{p(y|\theta_1, \theta_2^*, \theta_3)p(\theta_1, \theta_2^*, \theta_3)}{p(y|\theta_1, \theta_2, \theta_3)p(\theta_1, \theta_2, \theta_3)}\}. \tag{3.5}$$

7) Generate $U_2 \sim U(0, 1)$, if $U_2 \le \varsigma_2(\theta, \theta^*)$ and set $\theta = \theta^*$; otherwise, keep θ unchanged.

8) Simulate $\theta_3^* \sim N(\theta_3^{(t-1)}, \sigma_3^2)$.

9) Let $\theta^* = (\theta_1, \theta_2, \theta_3^*)$, and compute

$$\varsigma_3(\theta, \theta^*) = min\{1, \frac{p(y|\theta_1, \theta_2, \theta_3^*)p(\theta_1, \theta_2, \theta_3^*)}{p(y|\theta_1, \theta_2, \theta_3)p(\theta_1, \theta_2, \theta_3)}\}. \tag{3.6}$$

10) Generate $U_3 \sim U(0,1)$, if $U_3 \leq \varsigma_3(\theta, \theta^*)$ and set $\theta = \theta^*$; otherwise, keep θ unchanged.

11) Let $\theta^{(t)} = \theta$.

Here, N_{sim} is the number of simulations; θ_1^*, θ_2^* and θ_3^* are generated from the symmetric normal distribution with the updated mean $\theta_1^{(t-1)}, \theta_2^{(t-1)}$, and $\theta_3^{(t-1)}$ respectively; and then fixed variance σ_1, σ_2, and σ_3 are given positive constants.

Remark 1: In the construction of the ISC–MH algorithm, we only consider the estimation problem with three unknown parameters. However, the ISC-MH algorithm can be easily extended to estimate models with more parameters than three. The required computational cost and the tuning of the proposal's variances would increase with the dimension, which should be studied more carefully before application to significantly higher-dimensional problems.

Remark 2: The initial parameter vector θ_0 is sampled from uniform distributions in this paper. However, the ISC–MH algorithm is consistent with standard Markov chain Monte Carlo (MCMC) theory. Once the chain has reached stationarity after the burn–in period (the burn–in length is 5000 in the following simulations, which is large enough), the posterior estimates are independent of the initial values. We verified this by running the algorithm with several different random initial guesses, and the resulting posterior summaries were nearly identical.

4. Numerical results of the forward problem

4.1. Numerical results of Example 1

The following example will be considered.

Example 1

$$\begin{cases} \frac{\partial^\alpha u}{\partial t^\alpha} = Q\frac{\partial^2 u(x,t)}{\partial x^2} - u(x,t) - u(x,t-s) + G(x,t), \quad (x,t) \in (0,1)\times(0,2], \\ u(x,0) = te^x, \quad x \in [0,1], t \in [-s,0], \\ u(0,t) = t, \quad u(1,t) = te, \quad t \in (0,2]. \end{cases} \tag{4.1}$$

The expression in (4.1) has the exact solution $u(x,t) = te^x$, and

$$G(x,t) = \frac{t^{1-\alpha}}{\Gamma(2-\alpha)}e^x + (2t - s - Qt)e^x.$$

where we take $s = 1$ in this example.

For the forward problem, we will use (2.7)–(2.9) to solve (4.1). Define

$$E_\infty(h,\tau) = \max_{0\leq i\leq M, 0\leq k\leq N} |U_i^k - u(x_i, t_k)|,$$

as the maximum error, and

$$R_{h\tau} = log_2 \frac{E_\infty(h,\tau)}{E_\infty(h/2,\tau)}.$$

as the convergence order. We then calculate $R_{h\tau}$ with different h and τ.

To obtain Figures 1–3 for Example 1, we fix $\alpha = 0.5$, $Q = 2$, and $s = 1$; take $h = 1/16$, and $\tau = 1/1024$. Figures 1 and 2 provide the mesh surface of the exact solution and the numerical solution of Example 1, respectively. Figure 3 provides the mesh surface of the absolute values of the difference between the numerical solution and the exact solution of Example 1. From Figures 1 and 2, the exact solution and the numerical solution are very close at each grid, which are confirmed by the absolute values of the difference between the numerical solution and the exact solution at the grids provided by Figure 3. From Figure 3, we can see that the error is as small as the quantity order of 10^{-8}.

To obtain Table 1, we fix $Q = 2$ and $s = 1$, and α is taken to be 0.5 and 0.9. Table 1 provides the numerical results of the maximum error and the convergence order of solving for Example 1. When h is reduced to $h/2$, τ is reduced to $\tau/16$, and the maximum error is reduced to 1/16 of the original error. In Table 1, we provide two types of mesh grids . One is $h = \tau = 1/4$, $h = 1/8, \tau = 1/64$, and $h = 1/16, \tau = 1/1024$; the other is $h = \tau = 1/8$, $h = 1/16, \tau = 1/128$, and $h = 1/32, \tau = 1/2048$. However, all the numerical results show that the maximum error is reduced to 1/16 of the original error. So we can draw a conclusion that the spatial convergence order is 4.

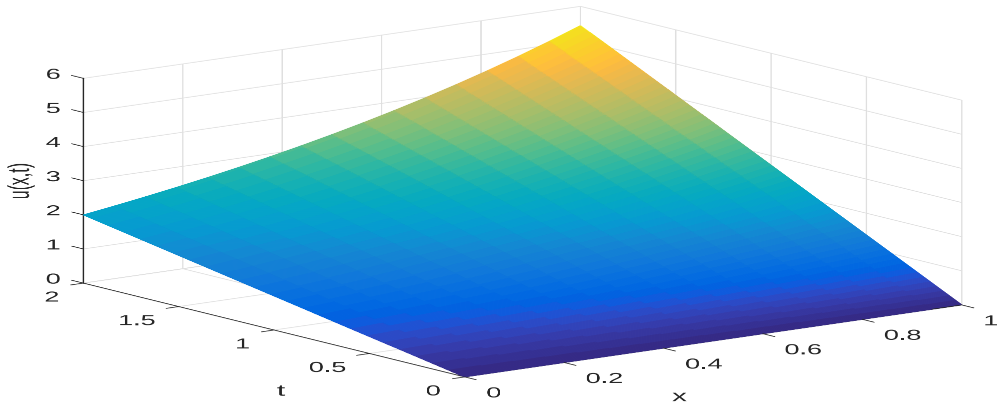

Figure 1. Exact solution of Example 1, where $\alpha = 0.5$, $Q = 2$, $s = 1$, $h = 1/16$, and $\tau = 1/1024$.

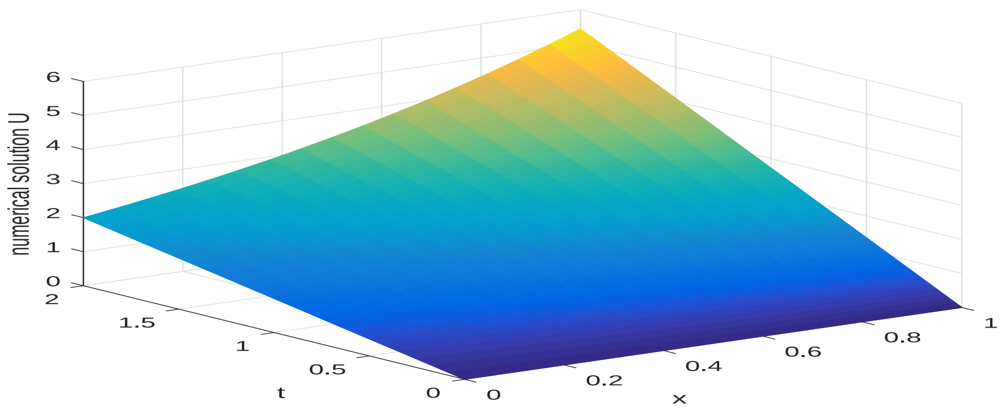

Figure 2. Numerical solution of Example 1, where $\alpha = 0.5$, $Q = 2$, $s = 1$, $h = 1/16$, and $\tau = 1/1024$.

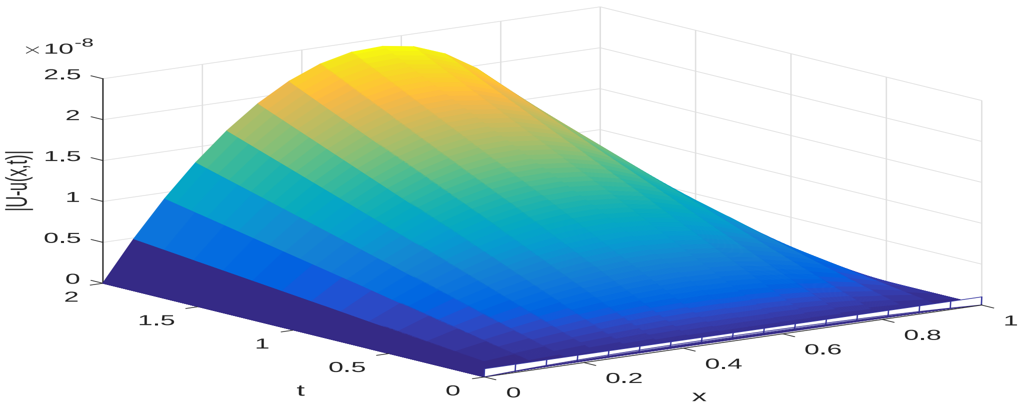

Figure 3. Absolute values of the difference between the numerical solution and the exact solution of Example 1, where $\alpha = 0.5$, $Q = 2$, $s = 1$, $h = 1/16$, and $\tau = 1/1024$.

Table 1. Numerical results of error and convergence for Example 1, where $Q = 2$ and $s = 1$.

	$\alpha = 0.5$ $E_\infty(h,\tau)$	$R_{h\tau}$	$\alpha = 0.9$ $E_\infty(h,\tau)$	$R_{h\tau}$
$h = \tau = 1/4$	6.099e-06	*	6.167e-06	*
$h = 1/8, \tau = 1/64$	3.818e-07	3.997	3.861e-07	3.997
$h = 1/16, \tau = 1/1024$	2.405e-08	3.989	2.431e-08	3.989
$h = \tau = 1/8$	3.818e-07	*	3.861e-07	*
$h = 1/16, \tau = 1/128$	2.405e-08	3.989	2.431e-08	3.989
$h = 1/32, \tau = 1/2048$	1.503e-09	3.999	1.520e-09	3.999

4.2. Numerical results of Example 2

Example 2

$$\begin{cases} \frac{\partial^\alpha u}{\partial t^\alpha} = Q\frac{\partial^2 u(x,t)}{\partial x^2} - u(x,t-s) + G(x,t), & (x,t) \in (0,1)\times(0,4], \\ u(x,0) = 2x^2(1-x)t^2, & x \in [0,1], t \in [-s,0], \\ u(0,t) = 0, \quad u(1,t) = 0, & t \in (0,4], \end{cases} \tag{4.2}$$

The expression in (4.2) has exact solution $u(x,t) = 2x^2(1-x)t^2$, and

$$G(x,t) = \frac{2\Gamma(3)}{\Gamma(3-\alpha)}x^2(1-x)t^{2-\alpha} - Q(4-12x)t^2 + 2x^2(1-x)(t-s)^2,$$

where $s = 1$ is considered.

Moreover, the compact difference scheme (2.7)–(2.9) is used to solve (4.2). To obtain Figures 4–6 of Example 2, we fix $\alpha = 0.7$, $Q = 5$, and $s = 1$; take $h = 1/32$, and $\tau = 1/2048$. Figures 4 and 5 provide the mesh surface of the exact solution and the numerical solution of Example 2, respectively. Figure 6 provides the mesh surface of the absolute values of the difference between the numerical solution and the exact solution of Example 2. In Figures 4 and 5, the exact solution and the numerical solution are very close at each grid, which are confirmed by the the absolute values of the difference between the numerical solution and the exact solution at the grids provided by Figure 6. From Figure 6, we can see that the error is as small as the quantity order of 10^{-6}.

To obtain Table 2, we fix $Q = 5$ and $s = 1$, and α is taken to be 0.3 and 0.7. Table 2 provides the numerical results of the maximum error and the convergence order of solving for Example 2. When h is reduced to $h/2$, τ is reduced to $\tau/16$, and the maximum error is reduced to 1/16 of the original error. In Table 2, we provide two types of mesh grid; one is $h = \tau = 1/4$, $h = 1/8, \tau = 1/64$, and $h = 1/16, \tau = 1/1024$; the other is $h = \tau = 1/8$, $h = 1/16, \tau = 1/128$, and $h = 1/32, \tau = 1/2048$. However, all the numerical results show that the maximum error is reduced to more than 1/16 of the original error. So we can draw a conclusion that the spatial convergence order is higher than 4.

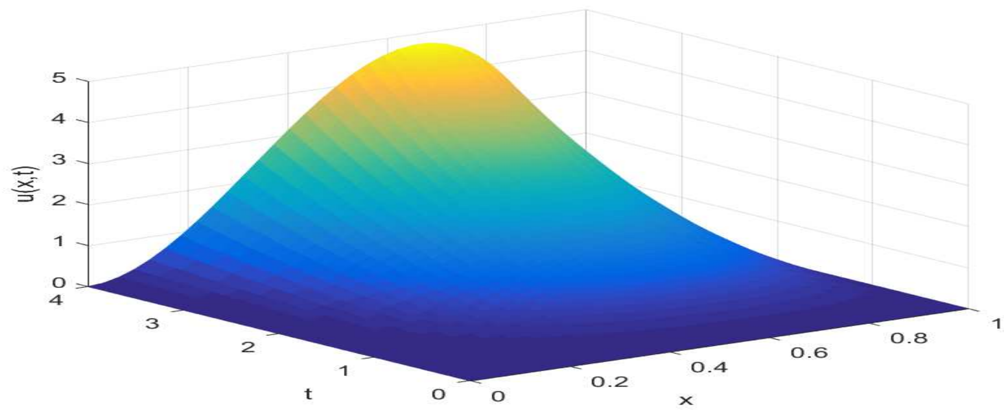

Figure 4. The exact solution of Example 2, where $\alpha = 0.7$, $Q = 5$, $s = 1$, $h = 1/32$, and $\tau = 1/2048$.

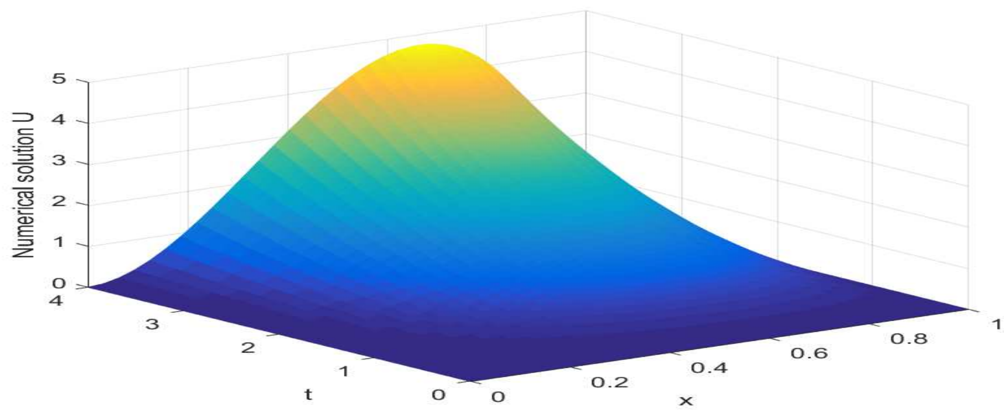

Figure 5. The numerical solution of Example 2, where $\alpha = 0.7$, $Q = 5$, $s = 1$, $h = 1/32$, and $\tau = 1/2048$.

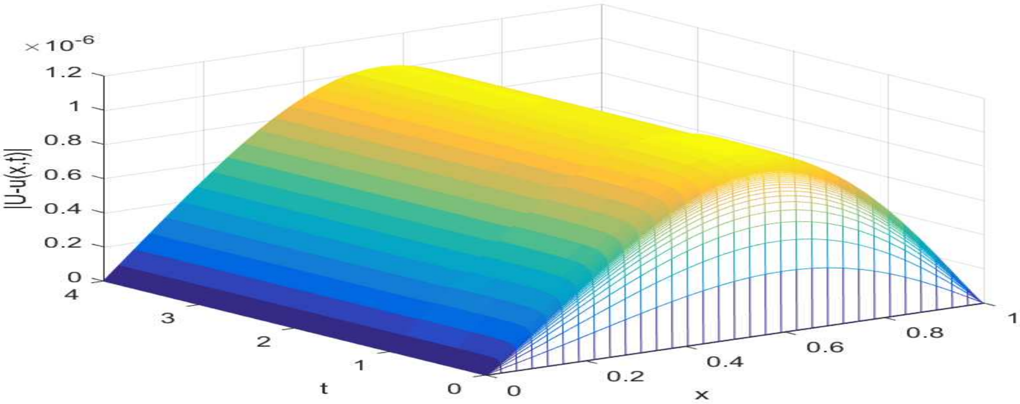

Figure 6. Absolute values of the difference between the numerical solution and the exact solution of Example 2, where $\alpha = 0.7$, $Q = 5$, $s = 1$, $h = 1/32$, and $\tau = 1/2048$.

Table 2. Numerical results of error and convergence for Example 2, where $Q = 5$ and $s = 1$.

	$\alpha = 0.3$		$\alpha = 0.7$	
	$E_\infty(h,\tau)$	$R_{h\tau}$	$E_\infty(h,\tau)$	$R_{h\tau}$
$h = \tau = 1/4$	1.198e-03	*	3.225e-03	*
$h = 1/8, \tau = 1/64$	1.292e-05	6.535	9.097e-05	5.148
$h = 1/16, \tau = 1/1024$	1.265e-07	6.675	2.541e-06	5.162
$h = \tau = 1/8$	3.935e-04	*	1.327e-03	*
$h = 1/16, \tau = 1/128$	4.141e-06	6.570	3.771e-05	5.137
$h = 1/32, \tau = 1/2048$	3.932e-08	6.719	1.033e-06	5.190

5. Numerical results of the inverse problem

5.1. Estimation results of Example 1

To obtain the observations Y, we fix $\alpha = 0.5$, $Q = 5$, and $s = 1$ in Eq (4.1). One can use the compact difference scheme (2.7)–(2.9) to numerically solve (4.1) first, where $M = N = 100$. With a fixed time $t = T = 2$, we sampled every fifth point (or every second point, or all points) from the numerical solutions $\{U_i^{N+1}\}, i = 0, 1, \cdots, M$. We then added the noise on each point, and the observations with length $n = 20$ ($n = 50$, $n = 100$) were obtained, where different values of σ were considered in (3.1), such as $\sigma = 0.05, 0.1, 0.5, 1$.

In the remainder of this paper, we fix the total simulation number to be N_{sim} = 10,000, and the number of burn–in samples is taken to be 5000 in the ISC-MH algorithm. (However, the burn–in length was determined by visually inspecting the trace plots of the MCMC chains, which showed good convergence before the 1000th iteration; the burn–in length could be 2000, 3000, 4000, 5000, and so on.) Moreover, we fixed $\sigma_1 = 0.1$, $\sigma_2 = 0.5$, and $\sigma_3 = 0.2$ to obtain Tables 3 and 4. However, different values are considered in Table 5 to evaluate the influence of σ_1, σ_2, and σ_3 on the ISC-MH algorithm. The initial value of the ISC-MH algorithm is taken as $\theta_0 = (\alpha_0, Q_0, s_0) = (\theta_1^{(0)}, \theta_2^{(0)}, \theta_3^{(0)}) \sim (U(0,1), U(0,10), U(0,2))$.

Table 3. Estimation results (mean, standard error, and 95% credible interval) of α, Q, and s in Example 1 under different values of noise σ, where the true values of the parameter are $\alpha = 0.5, Q = 5$, and $s = 1$.

		α	Q	s
$\sigma = 0.05$	Mean	0.4849	5.5990	0.9402
	SD	0.2807	2.7631	0.5581
	95%	[0.0516, 0.9440]	[0.9216, 9.5858]	[0.1184, 1.8748]
$\sigma = 0.1$	Mean	0.4860	5.6066	0.9407
	SD	0.2790	2.7503	0.5543
	95%	[0.0548, 0.9447]	[0.9425, 9.5749]	[0.1088, 1.8711]
$\sigma = 0.5$	Mean	0.4880	5.6287	0.9365
	SD	0.2810	2.7596	0.5586
	95%	[0.0528, 0.9468]	[0.9596, 9.5946]	[0.1092, 1.8724]
$\sigma = 1$	Mean	0.4868	5.6042	0.9454
	SD	0.2806	2.7525	0.5662
	95%	[0.0524, 0.9450]	[0.9415, 9.5751]	[0.1056, 1.8818]

Table 4. Numerical results (mean, standard error, and 95% credible interval) of α, Q, and s in Example 1 under different values of n, where the true values of the parameter are $\alpha = 0.5, Q = 5$, and $s = 1$.

		α	Q	s
$n = 20$	Mean	0.4871	5.6066	0.9492
	SD	0.2806	2.7503	0.5599
	95%	[0.0527, 0.9453]	[0.9425, 9.5749]	[0.1034, 1.8768]
$n = 50$	Mean	0.4881	5.6165	0.9508
	SD	0.2768	2.7577	0.5663
	95%	[0.0611, 0.9386]	[0.9366, 9.5774]	[0.0990, 1.8875]
$n = 100$	Mean	0.4856	5.6328	0.9430
	SD	0.2795	2.7600	0.5638
	95%	[0.0516, 0.9364]	[0.9645, 9.5995]	[0.1059, 1.8611]

First, we consider the impact of different σ on the ISC-MH algorithm in Table 3. So n is fixed to be 20, and σ is taken to be 0.05, 0.1, 0.5, and 1. The true values of the parameter to be estimated in (4.1) are taken to be $\alpha = 0.5, Q = 5$, and $s = 1$. The estimation results are shown together in Table 3. We also consider the impact of different values of n to the ISC-MH algorithm in Table 4, where $\sigma = 0.7$ is fixed, and n is taken to be 20, 50 and 100. From Tables 3 and 4, we can see that the ISC-MH algorithm can provide a good estimation for the parameter $\theta = (\alpha, Q, s)$ in the system of (3.1) together with (4.1).

Finally, we investigate the influence of σ_1, σ_2, and σ_3 on the ISC-MH algorithm. To obtain the estimation results in Table 5, we fix $n = 20$ and $\sigma = 0.5$. We can see that more accurate estimation of the parameter θ can be obtained when larger values of σ_1, σ_2, and σ_3 are given.

Table 5. Numerical results (mean, standard error, and 95% credible interval) of α, Q, and s in Example 1 under different values of σ_1, σ_2, and σ_3, where the true values of the parameter are $\alpha = 0.5$, $Q = 5$, and $s = 1$.

		α	Q	s
$\sigma_1 = 0.05$	Mean	0.4691	5.7937	0.9403
$\sigma_2 = 0.25$	SD	0.2842	2.4566	0.5578
$\sigma_3 = 0.1$	95%	[0.0437, 0.9375]	[1.6379, 9.4888]	[0.0910, 1.8530]
$\sigma_1 = 0.1$	Mean	0.4880	5.6287	0.9365
$\sigma_2 = 0.5$	SD	0.2810	2.7596	0.5586
$\sigma_3 = 0.2$	95%	[0.0528, 0.9468]	[0.9596, 9.5946]	[0.1092, 1.8724]
$\sigma_1 = 0.2$	Mean	0.4912	5.2213	0.9893
$\sigma_2 = 1$	SD	0.2845	2.7897	0.5614
$\sigma_3 = 0.4$	95%	[0.0521, 0.9447]	[0.7116, 9.5195]	[0.1162, 1.8924]

5.2. *Estimation results of Example 2*

To obtain the observations of Y, we fix $\alpha = 0.5, Q = 5$, and $s = 1$ in Eq (4.2). One can use the compact difference scheme of (2.7)–(2.9) to numerical solve (4.2) first, where $M = N = 100$. With a fixed time $t = T = 4$, we sampled every fifth point (or every second point, or all points) from the numerical solutions $\{U_i^{N+1}\}, i = 0, 1, \cdots, M$. We added the noise on each point, and the observations with length $n = 20$ ($n = 50, n = 100$) were obtained, where different values of σ considered in (3.1), such as $\sigma = 0.1, 0.5$, and 1.

In the following simulations, we fix the total simulation number to be $N_{sim} = 10{,}000$, and the number of burn–in samples is taken to 5000 in the ISC-MH algorithm, and we fix $\sigma_1 = 0.1$, $\sigma_2 = 0.5$, and $\sigma_3 = 0.2$ to obtain Tables 6 and 7. Different values are considered in Table 8 to evaluate the influence of σ_1, σ_2, and σ_3 on the ISC-MH algorithm. The initial value of the ISC-MH algorithm is taken to be $\theta_0 = (\alpha_0, Q_0, s_0) = (\theta_1^{(0)}, \theta_2^{(0)}, \theta_3^{(0)}) \sim (U(0, 1), U(0, 10), U(0, 2))$.

Table 6. Estimation results (mean, standard error, and 95% credible interval) of α, Q, and s in Example 2 under different values of noise σ, where the true values of the parameter are $\alpha = 0.5, Q = 5$, and $s = 1$.

		α	Q	s
$\sigma = 0.1$	Mean	0.4858	5.5989	0.9667
	SD	0.2790	2.7618	0.5505
	95%	[0.0545, 0.9445]	[0.9441, 9.5683]	[0.1388, 1.8873]
$\sigma = 0.5$	Mean	0.4842	5.6123	0.9574
	SD	0.2792	2.7677	0.5616
	95%	[0.0545, 0.9423]	[0.9216, 9.5823]	[0.1098, 1.8798]
$\sigma = 1$	Mean	0.4840	5.5989	0.9461
	SD	0.4840	2.7618	0.5629
	95%	[0.0542, 0.9420]	[0.9441, 9.5683]	[0.1107, 1.8946]

Table 7. Numerical results (mean, standard error, and 95% credible interval) of α, Q, and s in Example 2 under different values of n, where the true values of the parameter are $\alpha = 0.5, Q = 5$, and $s = 1$.

		α	Q	s
$n = 20$	Mean	0.4858	5.5824	0.9559
	SD	0.2790	2.7531	0.5608
	95%	[0.0545, 0.9445]	[0.9241, 9.5576]	[0.1068, 1.8830]
$n = 50$	Mean	0.4883	5.5829	0.9581
	SD	0.2812	2.7531	0.5598
	95%	[0.0536, 0.9482]	[0.9246, 9.5581]	[0.1123, 1.8841]
$n = 100$	Mean	0.4858	5.5824	0.9418
	SD	0.2790	2.7531	0.5588
	95%	[0.0545, 0.9445]	[0.9241, 9.5576]	[0.1080, 1.8844]

Table 8. Numerical results (mean, standard error, and 95% credible interval) of α, Q, and s in Example 2 under different values of σ_1, σ_2, and σ_3, where the true values of the parameter are $\alpha = 0.5, Q = 5$, and $s = 1$.

		α	Q	s
$\sigma_1 = 0.05$	Mean	0.4683	5.8960	0.9443
$\sigma_2 = 0.25$	SD	0.2852	2.4559	0.5556
$\sigma_3 = 0.1$	95%	[0.0416, 0.9391]	[1.5877, 9.5131]	[0.1074, 1.8541]
$\sigma_1 = 0.1$	Mean	0.4842	5.6123	0.9574
$\sigma_2 = 0.5$	SD	0.2792	2.7677	0.5616
$\sigma_3 = 0.2$	95%	[0.0545, 0.9423]	[0.9216, 9.5823]	[0.1098, 1.8798]
$\sigma_1 = 0.2$	Mean	0.4889	5.2550	0.9840
$\sigma_2 = 1$	SD	0.2830	2.7928	0.5616
$\sigma_3 = 0.4$	95%	[0.0565, 0.9460]	[0.6958, 9.5557]	[0.1075, 1.9040]

First, we consider the impact of different values of σ on the ISC–MH algorithm in Table 6. Here n is fixed to be 20, and σ is taken to be 0.1, 0.5, and 1. The true values of the parameter to be estimated in (4.2) are taken to be $\alpha = 0.5, Q = 5$, and $s = 1$. The estimation results are shown together in Table 6. We also consider the impact of different values of n to the ISC–MH algorithm in Table 7, where $\sigma = 0.7$ is fixed, and n is taken to be 20, 50, and 100. From Tables 6 and 7, we can see that the ISC-MH algorithm can provide well estimation for the parameter $\theta = (\alpha, Q, s)$ in the system of (3.1) together with (4.2).

Finally, we also investigate the influence of σ_1, σ_2, and σ_3 on the ISC–MH algorithm. To obtain the estimation results in Table 8, we fix $n = 20$ and $\sigma = 0.5$. We can see that more accurate estimation of the parameter θ can be obtained when bigger values of σ_1, σ_2, and σ_3 are given.

6. Conclusions

The paper provides a compact difference scheme to discretize the fractional delay diffusion equation, and then considers the ISC-MH algorithm to estimate the unknown parameter of the model. For the forward problem, we also provide some results about the convergence and stability of the numerical scheme. For the inverse problem, the unknown parameter can be the fractional order α, the diffusion coefficient Q, and the time delay s. Finally, numerical tests of two examples were considered to test the performance of the compact difference scheme, and the estimation efficiency of the ISC-MH algorithm.

Use of AI tools declaration

The authors declare they have not used Artificial Intelligence (AI) tools in the creation of this article.

Acknowledgments

This work is supported by the National Natural Science Foundation of PR China (Grant No. 71974204).

Conflict of interest

The authors declare there are no conflicts of interest.

References

1. I. Podlubny, *Fractional Differential Equations*, Academic Press, New York, 1999. https://doi.org/10.1016/s0076-5392(99)x8001-5
2. R. Metzler, J. Klafter, The random walk's guide to anomalous diffusion: A fractional dynamics approach, *Phys. Rep.*, **339** (2000), 1–77. https://doi.org/10.1016/S0370-1573(00)00070-3
3. J. Bouchaud, A. Georges, Anomalous diffusion in disordered media: Statistical mechanisms, models and physical applications, *Phys. Rep.*, **195** (1990), 127–293. https://doi.org/10.1016/0370-1573(90)90099-N
4. Z. Sun, X. Wu, A fully discrete difference scheme for a diffusion-wave system, *Appl. Numer. Math.*, **56** (2006), 193–209. https://doi.org/10.1016/j.apnum.2005.03.003
5. G. Gao, Z. Sun, A compact finite difference scheme for the fractional sub-diffusion equations, *J. Comput. Phys.*, **230** (2011), 586–595. https://doi.org/10.1016/j.jcp.2010.10.007
6. N. Zhang, W. Deng, Y. Wu, Finite difference/element method for a two-dimensional modified fractional diffusion equation, *Adv. Appl. Math. Mech.*, **4** (2012), 496–518. https://doi.org/10.4208/aamm.10-m1210
7. J. Sun, W. Deng, D. Nie, Numerical approximations for the fractional Fokker-Planck equation with two-scale diffusion, *J. Sci. Comput.*, **91** (2022), 34. https://doi.org/10.1007/s10915-022-01812-z

8. Q. Wang, Numerical solutions for fractional kdv-burgers equation by adomian decomposition method, *Appl. Math. Comput.*, **182** (2006), 1048–1055. https://doi.org/10.1016/j.amc.2006.05.004
9. H. Mesgarani, A. Beiranvand, Y. E. Aghdam, The impact of the Chebyshev collocation method on solutions of the time-fractional Black-Scholes, *Math. Sci.*, **15** (2021), 137–143. https://doi.org/10.1007/s40096-020-00357-2
10. M. Stynes, E. O'Riordan, J. L. Gracia, Error analysis of a finite difference method on graded meshes for a time-fractional diffusion equation, *SIAM J. Numer. Anal.*, **55** (2017), 1057–1079. https://doi.org/10.1137/16M1082329
11. J. Shen, Z. Sun, R. Du, Fast finite difference schemes for time-fractional diffusion equations with a weak singularity at initial time, *East Asian J. Appl. Math.*, **8** (2018), 834–858. https://doi.org/10.4208/eajam.010418.020718
12. N. Kopteva, Error analysis of the L1 method on graded and uniform meshes for a fractional-derivative problem in two and three dimensions, *Math. Comput.*, **88** (2019), 2135–2155. https://doi.org/10.1090/mcom/3410
13. N. Kopteva, X. Meng, Error analysis for a fractional-derivative parabolic problem on quasi-graded meshes using barrier functions, *Phys. Rep.*, **58** (2020), 1217–1238. https://doi.org/10.1137/19M1300686
14. X. Meng, M. Stynes, Barrier function local and global analysis of an L1 finite element method for a multiterm time-fractional initial-boundary value problem, *J. Sci. Comput.*, **84** (2020), 5. https://doi.org/10.1007/s10915-020-01250-9
15. H. Chen, M. Stynes, Using complete monotonicity to deduce local error estimates for discretisations of a multi-term time-fractional diffusion equation, *Comput. Methods Appl. Math.*, **22** (2022), 15–29. https://doi.org/10.1515/cmam-2021-0053
16. D. Li, H. Liao, W. Sun, J. Wang, J. Zhang, Analysis of L1-Galerkin FEMs for time fractional nonlinear parabolic problems, *Commun. Comput. Phys.*, **24** (2018), 86–103. https://doi.org/10.4208/cicp.OA-2017-0080
17. H. Liao, W. Mclean, J. Zhang, A discrete Gronwall inequality with applications to numerical schemes for subdiffusion problems, *SIAM J. Numer. Anal.*, **57** (2019), 218–237. https://doi.org/10.1137/16M1175742
18. L. Li, B. Zhou, X. Chen, Z. Wang, Convergence and stability of compact finite difference method for nonlinear time fractional reaction–diffusion equations with delay, *Appl. Math. Comput.*, **337** (2018), 144–152. https://doi.org/10.1016/j.amc.2018.04.057
19. D. Li, W. Sun, C. Wu, A novel numerical approach to time-fractional parabolic equations with nonsmooth solutions, *Numer. Math. Theory Methods Appl.*, **14** (2021), 355–376. https://doi.org/10.4208/nmtma.OA-2020-0129
20. D. Li, H. Qin, J. Zhang, Sharp pointwise in time error estimate of L1 scheme for nonlinear subdiffusion equation, *J. Comput. Math.*, **42** (2024), 662–678. https://doi.org/10.4208/jcm.2205-m2021-0316

21. M. Li, B. Zhou, M. Zhang, W. Gu, Solvability and convergence analysis of a transformed L1 finite difference scheme for TFMBE models without slope selection, *J. Differ. Equ. Appl.*, **30** (2024), 361–376. https://doi.org/10.1080/10236198.2023.2290510

22. Y. Han, X. Huang, W. Gu, B. Zheng, Linearized transformed L1 finite element methods for semi-linear time-fractional parabolic problems, *Appl. Math. Comput.*, **458** (2023), 128242. https://doi.org/10.1016/j.amc.2023.128242

23. G. Pang, L. Lu, G. E. Karniadakis, fPINNs: Fractional physics-informed neural networks, *SIAM J. Sci. Comput.*, **41** (2019), A2603–A2626. https://doi.org/10.1137/18M1229845

24. J. Shi, X. Liu, X. Yang, Data-driven solutions and parameter estimation of the high-dimensional time-fractional reaction-diffusion equations using an improved fPINN method, *Nonlinear Dyn.*, **113** (2025), 9577–9604. https://doi.org/10.1007/s11071-024-10786-6

25. R. Zhang, F. Li, J. Liu, LT-PINNs: Physics-informed neural networks based on Laplace transform for solving Caputo-type fractional partial differential equations, *Chin. Phys. B*, **35** (2026), 030201. https://doi.org/10.1088/1674-1056/adf827

26. B. Yu, X. Y. Jiang, H. T. Qi, An inverse problem to estimate an unknown order of a Riemann-Liouville fractional derivative for a fractional Stokes' first problem for a heated generalized second grade fluid, *Acta Mech. Sin.*, **31** (2015), 153–161. https://doi.org/10.1007/s10409-015-0408-7

27. R. Malti, S. Victor, A. Oustaloup, H. Garnier, An optimal instrumental variable method for continuous-time fractional model identification, *IFAC Proc. Vol.*, **41** (2008), 14379–14384. https://doi.org/10.3182/20080706-5-KR-1001.02436

28. B. Zhang, Y. Tang, J. Zhang, Y. Lu, Coefficients and orders identification of fractional order systems based on block pulse functions through two-stage algorithm, *J. Dyn. Syst. Meas. Control*, **144** (2022), 071001. https://doi.org/10.1115/1.4054126

29. T. D. Fadale, A. V. Nenarokomov, A. F. Emery, Uncertainties in parameter estimation: The inverse problem, *Int. J. Heat Mass Transf.*, **38** (1995), 511–518. https://doi.org/10.1016/0017-9310(94)00175-U

30. N. Z. Sun, W. G. Yeh, A stochastic inverse solution for transient groundwater flow: Parameter identification and reliability analysis, *Water Resour. Res.*, **28** (1992), 3269–3280. https://doi.org/10.1029/92wr00683

31. H. S. Hoang, R. Baraille, O. Talagrand, P. DeMey, Approximate Bayesian approach to non-Gaussian estimation in a linear model with dependent state and noise vectors, *Appl. Math. Optim.*, **43** (2001), 203–220. https://doi.org/10.1007/s00245-001-0005-y

32. M. A. Beaumont, W. Zhang, D. J. Balding, Approximate Bayesian computation in population genetics, *Genetics*, **162** (2002), 2025–2035. https://doi.org/10.1093/genetics/162.4.2025

33. M. A. Beaumont, J. M. Cornuet, J. M. Marin, C. P. Robert, Adaptive approximate Bayesian computation, *Biometrika*, **96** (2009), 983–990. https://doi.org/10.1093/biomet/asp052

34. T. Toni, D. Welch, N. Strelkowa, A. Ipsen, M. P. H. Stumpf, Approximate Bayesian computation scheme for parameter inference and model selection in dynamical systems, *J. R. Soc. Interface*, **6** (2009), 187–202. https://doi.org/10.1098/rsif.2008.0172

35. J. Kaipio, E. Somersalo, *Statistical and Computational Inverse Problems*, Springer, New York, 2005. https://doi.org/10.1007/b138659

36. W. Gu, F. Wei, M. Li, Parameter estimation for a type of fractional diffusion equation based on compact difference scheme, *Symmetry*, **14** (2022), 560. https://doi.org/10.3390/sym14030560

37. W. Zhang, W. Gu, Parameter estimation for several types of linear partial differential equations based on Gaussian processes, *Fractal Fract.*, **6** (2022), 433. https://doi.org/10.3390/fractalfract6080433

38. W. Zhang, W. Gu, Machine learning for a class of partial differential equations with multi-delays based on numerical Gaussian processes, *Appl. Math. Comput.*, **467** (2024), 128498. https://doi.org/10.1016/j.amc.2023.128498

39. W. Gu, Y. Zhou, X. Ge, A compact difference scheme for solving fractional neutral parabolic differential equation with proportional delay, *J. Funct. Spaces*, **2017** (2017), 3679526. https://doi.org/10.1155/2017/3679526

40. W. Gu, Investigations for a type of variable coefficient fractional subdiffusion equation with multidelay, *J. Funct. Spaces*, **2020** (2020), 6964159. https://doi.org/10.1155/2020/6964159